Gliding towards an understanding of the origin of flight in bats

Abigail E. Burtner[1], David M. Grossnickle[1,2], Sharlene E. Santana[1], Chris J. Law[1,3*]

[1]Department of Biology and Burke Museum of Natural History and Culture, University of Washington, Seattle WA 98195; [2]Natural Sciences Department, Oregon Institute of Technology, Klamath Falls, OR 97601; [3]Department of Integrative Biology, University of Texas, Austin, TX.

*Corresponding Author: Chris J. Law

Email address: cjlaw@uw.edu

Abstract

Bats are the only mammals capable of powered flight and have correspondingly specialized body plans, particularly in their limb morphology. The origin of bat flight is still not fully understood due to an uninformative fossil record but, from the perspective of a functional transition, it is widely hypothesized that bats evolved from gliding ancestors. Here, we test predictions of the gliding-to-flying hypothesis of the origin of bat flight by using phylogenetic comparative methods to model the evolution of forelimb and hindlimb traits on a dataset spanning four extinct bats and 231 extant mammals with diverse locomotor modes. Our results reveal that gliders exhibit adaptive trait optima (1) toward relatively elongate forelimbs that are intermediate between those of bats and non-gliding arborealists, and (2) toward relatively narrower but not longer hindlimbs that are intermediate between those of non-gliders and bats. We propose a hypothetical adaptive landscape based on limb length and width optimal trends derived from our modeling analyses. Our results support a hypothetical evolutionary pathway

wherein glider-like postcranial morphology precedes a bat-like morphology adapted to powered-flight, setting a foundation for future developmental, biomechanical, and evolutionary research to test this idea.

Introduction

Powered flight has evolved at least four times over the course of organismal evolution, consistently serving as a gateway to ecomorphological and species diversification (Heard and Hauser 1995; Hunter 1998; Jetz et al. 2012; Nicholson et al. 2014). As the only mammals capable of powered flight, bats have correspondingly specialized body plans that include highly derived limbs. These specialized morphologies are understood to be the result of adaptations for the demands of flight; the skeletal elements of bat forelimbs are elongated to support flight membranes and increase aerodynamic efficiency, whereas bat hindlimbs are not only specialized for hanging and catching prey in flight (Norberg 1990; Gunnell and Simmons 2005; Giannini 2012), but also contribute to flight itself (Cheney et al. 2014).

The evolutionary origin of flight in bats remains a subject of ongoing research and debate due to an uninformative fossil record linking bats to their non-flying ancestors. Nevertheless, bat flight is widely hypothesized to be the result of an ancestral “trees-down” transition from non-gliding tree-dweller (hereafter, ‘arborealist’) to glider to flyer (Norberg 1985B; Bishop 2008; Simmons et al. 2008), although this idea has not been tested using phylogenetic comparative methods. It should be noted that all phylogenomic evidence shows that bats are not closely related to any extant glider (Upham et al., 2019; Álvarez-Carretero et al., 2022); bats are nested within Laurasiatheria where neighboring clades are predominantly adapted to terrestrial

46 locomotion. Laurasiatheria is far from other placental gliders, including dermopterans and
47 rodents, located in the Eucarchontoglires superorder.

48 Following the arborealist-to-glider-to-flier hypothesis, the ancestors of bats–which
49 originated about 70-60 million years ago (Teeling et al. 2000; Upham et al. 2019; Álvarez-
50 Carretero et al. 2022)–are hypothesized to have evolved more elongated limbs, followed by
51 patagia (wing membranes) on the armwing to facilitate gliding, and finally membranes in the
52 handwing to enable powered flight. The armwing consists of stylopodal (i.e., humerus) and
53 zeugopodal (i.e., ulna and radius) bones, while the handwing consists of autopodal bones (i.e.,
54 the metacarpals and phalanges). The evolution of the handwing is thought to be the key
55 innovation that catalyzed bats' adaptive radiation (Vaughan 1970; Sears et al. 2006; Amador et
56 al. 2019), resulting in the evolution of over 1,500 extant species (Simmons and Cirranello
57 2022B).

58 Previous work has examined many biological features associated with the evolution of
59 bat flight, such as sensory adaptations (e.g., echolocation or vision), aerodynamics (e.g., aerofoil
60 and flight performance), ecology (e.g., diet, habitat, roosting), and development (e.g., patagia
61 development and digit elongation) (Bishop 2008; Cooper and Tabin 2008; Giannini 2012;
62 Anthwal et al., 2023; Feigin et al., 2023). Morphological approaches to understanding the origin
63 of bat flight further include analyses of skeletal dimensions in the context of development
64 (Adams 1992, 2008; Sears et al. 2006; Nojiri et al. 2023), biomechanics (Swartz et al. 1992;
65 Swartz 1997; Swartz and Middleton 2008), and functional morphology (Vaughan 1970). These
66 studies often focus on aspects of the bat forelimb (e.g., Amador et al. 2019) or hindlimb (e.g.,
67 Riskin et al. 2005), but seldom both in tandem in a phylogenetic context (but see Swartz and
68 Middleton 2008 and Nojiri et al. 2023). Here, we test predictions based on the gliding-to-flying

69 hypothesis of the origin of bat flight by modeling the evolution of forelimb and hindlimb traits
70 on a dataset spanning four extinct bats and 231 extant mammals with diverse locomotor modes
71 including ground-dwellers, arborealists, gliders, and flyers.

72 Following the arborealist-to-glider-to-bat hypothesis, we test two predictions regarding
73 the evolution of limb morphologies using an Ornstein-Uhlenbeck evolutionary model-fitting
74 approach. First, we predict that selection will lead the forelimb skeletal traits of arborealists,
75 gliders, and bats towards three separate adaptive trait optima/attractors (i.e., θ parameters of
76 fitted OU models, which are commonly interpreted as the locations of adaptive peaks in
77 morphospace; hereafter "optima"), where the glider forelimb optimum will be intermediate in
78 value to those of arborealists and bats. If supported, this demonstrates that glider morphology
79 may fall on an intermediate adaptive peak between bat and arborealist morphologies.
80 Specifically, we predict wider and longer skeletal element optima values progressing from
81 arborealists to gliders to bats. Relatively longer bones (especially in the handwing) and larger-
82 diameter bones (especially in combination with thinner, highly mineralized walls), may give bats
83 enough resistance to torsion during powered flight (Swartz et al. 1992) while still increasing their
84 patagia area. Glider optima with intermediate forelimb length and width optima between
85 arborealist and bat optima may represent an intermediate adaptive zone between the anatomical
86 adaptations required for tree-dwelling (Cartmill 1985) and those required for powered flight
87 (Norberg 1990). Support for this prediction would suggest selective pressures for flight
88 influenced the evolution of bat forelimb skeletal elements from glider-like forelimbs.

89 Second, we predict that bat hindlimb optima will exhibit a distinct trait optimum (i.e.,
90 adaptive peak) separate from ground-dwelling, arboreal, and gliding mammals. Previous work
91 has considered bat hindlimbs to be "reduced" in size (e.g., Farnum et al. 2008; Simmons et al.

2008; Louzada et al. 2019), whereas gliders exhibit relatively lengthened hindlimbs (Grossnickle et al. 2020; Linden et al. 2023; Rickman et al. 2023). Therefore, the relative lengths and widths of the hindlimb bones are not well characterized between these aerial groups as well as in relation to arborealists. Here, we aim to identify where bat hindlimb adaptive optima lie relative to other mammals. Specifically, we predict narrower and longer skeletal element optima values progressing from arborealists to bats and gliders. We predict overlapping hindlimb optima between gliders and bats because relatively longer and lower-diameter hindlimb bones in both groups relative to arborealists and ground-dwellers may decrease weight while still generating lift. Support for this prediction would suggest that shared selective pressures for less-quadrupedal motion (i.e., as gliding and flying both incorporate hindlimbs into the wing membrane) influenced the evolution of bat hindlimb skeletal elements from ancestors with glider-like hindlimbs. Overall, this study offers the first phylogenetically informed test of morphological data to investigate whether the adaptive optima of arborealists, gliders, and flyers illustrate a possible route across adaptive peaks in the evolution of mammalian flight.

Materials & Methods

Morphological Data

We compiled linear measurements of 14 forelimb and 15 hindlimb traits (Fig. 1) from 231 extant mammals (1–2 specimens per species) across 21 orders (78% of mammalian orders) and 73 families (47% of mammalian families). Of these, 26 representative species of bats (48 specimens) were measured for the flyer group. Linear measurements were obtained from specimens held at the Burke Museum of Natural History and Culture or from previously published work (Chen and Wilson 2015; Grossnickle et al. 2020; Weaver and Grossnickle 2020;

Pevsner et al. 2022). All specimens measured for this study were fully mature, determined by the closure of exoccipital–basioccipital and basisphenoid–basioccipital sutures on the cranium and ossification of all vertebrae and limb bones. Specimens were a mixture of male, female, and unknown sexes. We size-corrected all linear measurements by calculating log-shape ratios of each trait measurement (Mosimann 1970) by $\log_{10}$-transforming the mean trait value divided by the cube root of body mass prior to running all statistical analyses. Unfortunately, most specimens lacked accompanying body mass data; therefore we compiled species-level body mass data from the PanTHERIA database (Jones et al. 2009) and the *Handbook of the Mammals of the World* book series (Wilson and Mittermeier 2009).

We also collected the 29 measurements for four extinct bats (*Onychonycteris finneyi, Icaronycteris index, Hassianycteris messelensis, and Tachypteron franzeni*) using ImageJ (Schneider et al. 2012) on published full-body images that include scale bars (Storch et al. 2002; Gunnell and Simmons 2005; Simmons et al. 2008). We estimated the body masses of extinct bats using a linear regression between the body mass and geometric mean of all linear measurements from the extant bats of our dataset and used those body mass estimations to size-correct our fossil data again using log-shape ratios. We included fossil bats in our morphological dataset because, although extinct bats have a high degree of morphological similarity to extant bats (Norberg 1985B; Bishop 2008; Simmons et al. 2008), the fossil bat data may alter model estimations of the adaptive zone between flyers and gliders in an informative way. For example, the inclusion of fossils may make the flyer-glider trait optima more similar or more disparate by adding more phylogenetic history information and thus inform the understanding of the adaptive landscape underlying the evolution of mammalian flight.

To visualize the distribution of locomotor groups in the forelimb and hindlimb morphospaces, we performed principal component analyses (PCA) of the morphometric data using the *princomp* function in the *R* package *stats* (R Core Team 2021).

Locomotor Data

We categorized species into four locomotor groups: ground dwellers (n = 117), arborealists (n = 71), gliders (n = 16), and flyers (n = 27) following previous work (Chen and Wilson 2015; Grossnickle et al. 2020; Weaver and Grossnickle 2020; Pevsner et al. 2022). The ground-dwelling mammals included diverse ambulatory, cursorial, saltatorial, and fossorial taxa. This 'catch-all' category was intentional as we are interested in investigating the arboreal to gliding to flying specialization trends only. Our arborealist category was also broad in that it includes both fully arboreal (tree-dwelling) and scansorial taxa. Gliders included tree-dwelling mammals with derived morphologies (i.e., patagia and elongated limbs) for gliding locomotion (Grossnickle et al. 2020). Flyers included bats only.

Phylogenetic Comparative Analyses

We used evolutionary models (Hansen 1997; Butler and King 2004) to examine the influence of locomotor modes on the evolution of forelimb and hindlimb morphologies in our extant-only and extant+extinct datasets. We first tested the hypothesis that locomotor modes influenced the evolution of the forelimb and hindlimb using multivariate evolutionary models on our extant datasets (Butler & King, 2004; Hansen, 1997) in the R package mvMORPH (Clavel et al., 2015). To reduce the dimensions of our data, we conducted a principal component analysis (PCA) on our 14-trait forelimb dataset and 15-trait hindlimb dataset. We retained the first three

principal components (PCs) of our forelimb dataset (91.8% of the forelimb variation) and hindlimb dataset (85.3% of hindlimb variation). We then fit six multivariate models to the scores of these three PCs. We fit a multivariate Brownian motion model (mvBM), which models trait variance in a random walk over time; a single-regime multivariate Ornstein-Uhlenbeck model (mvOU1), in which scores of each PC evolve towards a single trait optimum (θ parameter of OU models), giving a single mean optimum for all locomotor groups; and multivariate OU models (mvOUM) with a given number of optima corresponding to selective regimes (based on locomotor modes). To test our hypotheses on overall limb evolution, we fit a four-peak OU model ($mvOUM_{loc4}$) for distinct optima among ground-dweller, arborealist, glider, and flyer regimes. To test alternative hypotheses, we fit three three-peak models ($mvOUM_{loc3a\text{-}c}$) with distinct combinations of the four locomotor groups. The $mvOUM_{loc3a}$ model tests for distinct optima among ground-dweller, arborealist, and a combined glider-flyer regimes. The $mvOUM_{loc3b}$ model tests for distinct optima among ground-dweller, combined arborealist-glider, and flyer regimes. The $mvOUM_{loc3c}$ model tests for distinct optima among a combined ground-dweller-arborealist, glider, and flyer regimes.

To account for uncertainty in phylogenetic topology and the ancestral character states (Fig. 1), we used the *make.simmaps* function in the *R* package *phytools* (Revell 2012) to simulate 10 stochastic character maps across 1,000 tree topologies randomly drawn from the posterior distribution of "completed" trees from Upham et al. (2019), resulting in 10,000 character maps of locomotory regimes. We randomly sampled 250 trees and fit all six models to these trees. We assessed relative model support using small sample corrected Akaike weights (AICcW). Models with ΔAICc scores less than two were considered supported and interpreted as evidence of locomotor groups influencing species' adaptive zones. We acknowledge that using a subset of

183 PCs instead of the full dataset could bias our results (D. C. Adams & Collyer, 2018; Uyeda et al.,
184 2015). However, our results remained consistent when we increased the number of PCs in our
185 model-fitting analyses to the first four or five PCs. Further, we used simulations to assess
186 whether we had adequate power to accurately distinguish between complex mvOU models from
187 Brownian motion (Boettiger et al., 2012).

188 If the $mvOUM_{loc4}$ model is best-supported, we interpreted this as each locomotor regime
189 having its own distinct adaptive optimum. This result alone does not provide evidence for the
190 evolutionary origin of bats. However, if gliders are located at an optimum between arborealists
191 and flyers (i.e., if arborealist < glider < flyer optima or arborealist > glider > flyer optima), there
192 is support for an evolutionary "pathway" between the two locomotor modes relative to an
193 ancestral arborealist or ground-dwelling state (i.e., one could theoretically bridge adaptive peaks
194 via these pathways). Therefore, if the optima gradually change in value (as opposed to random
195 changes in value) from arborealists to gliders to bats, our hypothesis that bats evolved from
196 gliding ancestors is supported.

197 If the $mvOUM_{loc3a}$ model is best-supported, we interpret this as gliders+flyers having a
198 shared adaptive optimum and arborealists and ground-dwellers having their own distinct
199 evolutionary optima. This model provides the clearest support for flyers evolving from gliding
200 ancestors because lineages of both groups are evolving towards the same shared adaptive optima.
201 Therefore, if this model best fit the data, our hypothesis is supported.

202 If the $mvOUM_{loc3b}$ model is best-supported, we interpret this as arborealists+gliders
203 having a shared adaptive optimum and flyers and ground-dwellers having their own distinct
204 evolutionary optima. There is phylogenetic justification for this grouping because all gliders
205 evolved from ancestrally arboreal groups (e.g., gliding squirrels evolved from tree squirrels; see

206 tree in Fig. 1). These groups are similar to the 4-group model in that if arborealists+gliders have
207 an optimum between those of ground-dwellers and flyers, there is support for an evolutionary
208 "pathway" between the two locomotor modes relative to an ancestral ground-dwelling state.
209 Finally, if $mvOUM_{loc3c}$ model is best-supported, we interpret this as ground-
210 dwellers+arborealists having a shared adaptive optimum and flyers and gliders having their own
211 distinct evolutionary optima. As with the $mvOUM_{loc4}$ and $mvOUM_{loc3b}$ models, if gliders have an
212 optimum between those of ground-dwellers+arborealists and flyers, there is support for an
213 adaptive "pathway" between the two locomotor modes relative to an ancestral arborealist or
214 ground-dwelling state, providing evidence for our hypothesis that flyers evolved from gliding
215 ancestors.
216 We also examined the influence of locomotor modes on the evolution of each individual
217 forelimb and hindlimb trait in our extant-only and extant+extinct datasets using univariate
218 evolutionary models. For each of the 29 traits, we fit a Brownian motion model (BM), a single-
219 optimum Ornstein-Uhlenbeck model (OU1), and four multiple-peak OU (OUM) models. The
220 OUM models included OUM_{loc4}, OUM_{loc3a}, OUM_{loc3b}, and OUM_{loc3c}, featuring the same
221 locomotor regimes as the multivariate mvMORPH models. All models were fit using the *R*
222 package *OUwie* (Beaulieu et al. 2012). We applied a single selection parameter (α) and rate
223 parameter (σ^2) across all selective regimes while allowing optima (θ) to vary between regimes
224 (Hansen 1997; Butler and King 2004). For traits in which an OUM model was the best-supported
225 model, we computed 95% confidence intervals using parametric bootstrapping of the model
226 parameters with the *OUwie.boot* function in the *R* package *OUwie* (Beaulieu et al. 2012). We
227 randomly sampled 100 of our character maps and performed 10 bootstrap replicates per
228 stochastic character map sampled.

We repeated the above multivariate and univariate model fitting approaches on a merged dataset that includes extant species and the four fossil species. All four models were fit across 50 stochastically mapped trees to account for uncertainty in the ancestral character states. We manually placed the four extinct bats on the phylogeny as a polytomy with extant bats at 69.8 MYA.

Results

Forelimb morphospace and evolutionary model-fitting

PC1 explains 81.5% of the forelimb variation and separates flyers (both extant and extinct) from the remaining three locomotor modes (Fig. 2a; Table S1a). PC1 also slightly separates gliders from arborealists and ground-dwellers. This axis describes the relative lengths of the armwing (humerus, radius, ulna) and the handwing (metacarpals and phalanges). PC1 varies across relatively shorter (-PC1) to elongate (+PC1) bones, revealing a trend within the dataset in the elongation of multiple forelimb bone elements from arborealists to gliders to flyers. PC2 explains 7.8% of the morphological variation and primarily describes the relative widths of the long bones and hands. This variation of wide to narrow bones mostly occurs within locomotor groups, especially within the diverse ground-dweller group. PC3 explains 2.9% of the morphological variation with +PC3 dominated by metacarpal length, ulna olecranon length, and scapula height and -PC3 dominated by intermediate phalanx length and humerus distal width. Fossil bats overlap with extant bats in morphospace, which is consistent with the lack of transitional forms in the bat fossil record.

The $mvOUM_{loc3b}$ model, which assigns arborealists and gliders to the same regime, was the best-fitting model for the extant multivariate forelimb dataset (PCs 1-3) (AICcW = 0.99,

Table 1a). Distinct optima were supported for these three locomotor groups, with PC1 and PC2 optima scores increasing in value from ground-dweller to arborealist+glider to flyer hindlimbs (Fig. 2c). Repeating the multivariate model-fitting with the addition of the four extinct flyer species yielded a $mvOUM_{loc4}$ model as the best fit (mAICcW = 0.99; Table S6a). However, the optima exhibited unrealistic magnitudes (Table S6b).

When we examined each forelimb trait individually using univariate models, we found that the OUM_{loc4} model was the best-fitting model for six of the 14 forelimb traits (AICcW = 0.51-1.00), OUM_{loc3b} was the best-fitting model for five traits (AICcW = 0.36-0.65), OUM_{loc3c} was the best fitting model for metacarpal length (AICcW = 0.63), and OUM_{loc3a} was the best-fitting model for ulna olecranon length (AICcW = 0.58; Table S2a). The OU1 model was the best fit for the proximal phalanx width of the third manual digit (AICcW = 0.51). Armwing (i.e., humerus and radius) length traits have optima (from the best-fitting OUM_{loc4} models) that gradually increase from ground-dwellers to arborealists to gliders to flyers; parametric bootstrapping revealed little to no overlap in the 95% confidence intervals of optima between most locomotor groups (Fig. 3b-c). Optima of armwing widths (from the best-fitting OUM_{loc3b} models) indicated that flyers exhibit relatively wider humeri at the distal end, proximal end, and mid-shaft compared to all other locomotor groups (Fig. 3g-i; Table S3a). Flyers exhibit relatively higher optima for handwing length traits (i.e., longer third manual metacarpal, proximal phalanx, and intermediate phalanx) than all other locomotor groups (Fig. 3d-f; Table S3a). For each, glider optima were intermediate between ground-dweller and arborealist optima. For handwing width traits, flyers exhibit relatively higher OUM_{loc3b} optima for metacarpal widths compared to all other locomotor groups (Fig. 3j), but no differences in proximal phalanx width as evidenced by OU1 support for this trait. An adaptive optimum for a flyer-glider combined group in the

275 OUM_{loc3a} models was supported for ulna olecranon length only (Table S2a). In total, however,
276 glider optima (in combination with arborealists) were between the 95% confidence intervals of
277 ground-dweller and flyer optima for all traits except scapula length/width, humerus proximal
278 width, and metacarpal width (Fig. 3a, 3g, 3j; Table S3a). For these last trait optima,
279 glider+arborealist optima were statistically the same as that of ground-dwellers while flyers
280 exhibited higher optima than all other locomotor groups (Fig. 3a, 3g, 3j; Table S3a).
281 Adding fossil flyers into forelimb model-fitting analyses yielded overall slightly more
282 support for OUM_{loc3a} models compared to extant-only modeling; scapula height and humerus
283 proximal width demonstrate support for a flyer-glider combined group (Table S4a). OUM_{loc4} and
284 OUM_{loc3b} models were still widely supported as the best-fitting model for six traits and five
285 traits, respectively; OU1 was still the best-fitting model for proximal phalanx width (Table S4a).
286 Overall, the length and width optima values for the forelimb were very similar between
287 extant+extinct and extant only-modeling (Table S5a).
288
289 *Hindlimb morphospace and evolutionary model-fitting*
290 PC1 explains 47.5% of hindlimb variation and more positive PC1 scores describe the
291 relative elongation (+PC1) of the fibula, metatarsal, and pedal proximal and intermediate
292 phalanges (Fig. 2b; Table S1b). PC1 slightly separates gliders and flyers, with gliders falling
293 towards +PC1 and flyers falling towards -PC1, indicating glider hindlimb autopodia are overall
294 more elongated than flyers'. Arborealists and ground-dwellers are spread across PC1. PC2
295 explains 17.8% of the variation, where +PC2 is associated with relatively lengthened pedal
296 proximal phalanges, intermediate phalanges, and ischium and -PC2 with relatively narrower
297 pedal proximal and intermediate phalanges. PC2 loosely separated ground-dwellers, arborealists,

298 and the glider-flyer group. PC3 explains 11.3% of the morphological variation with +PC3
299 dominated by ilium length, femur length, and fibula length and -PC3 dominated by metatarsal
300 width, intermediate phalanx width, and proximal phalanx width. These loadings show that
301 variation between the four locomotor groups mainly occurs throughout the hindlimb autopodia
302 region.

303 The $mvOUM_{loc4}$ model was the best-fitting model for the extant multivariate hindlimb
304 dataset (PCs 1-3) (AICcW = 0.92, Table 1b). Distinct optima were supported for the four
305 locomotor regimes, with PC1 and PC2 optima scores decreasing in value from ground-dweller to
306 arborealist to glider to flyer hindlimbs, albeit with overlap (Fig. 2d). Adding in the four extinct
307 flyer species yielded again the $mvOUM_{loc4}$ model as the best fit, and very little change in the
308 optima values (Table S6).

309 When we examined each hindlimb trait individually using univariate models, we found
310 that the OUM_{loc4} model was the best-fitting model for three of 15 traits, all of which were
311 hindlimb long bone lengths (AICcW = 0.33-0.60; Table S2b). Specifically, gliders have
312 relatively longer tibia and femoral optima compared to flyers and the other locomotor groups
313 (Fig. 4b-c, Table S3b). Fibula length was the third hindlimb trait supported by OUM_{loc4}, but
314 fibulae are rudimentary in bats. The OUM_{loc3a} model best fit three traits (AICcW = 0.36-0.52),
315 all of which were widths: femur shaft width, metatarsal width, and pedal proximal phalanx width
316 (Table S3b). Parametric bootstrapping of these OUM_{loc3a}-supported models revealed that the
317 glider-flyer group had relatively narrower femur shafts, metatarsals, and pedal proximal
318 phalanges optima than the other locomotor groups (Fig. 4f, i, j; Table S3b). The OUM_{loc3b} model
319 was the best-fitting model for four of the 15 traits (AICcW = 0.44-0.71): ilium, ischium,
320 metatarsal, and intermediate proximal phalanx length (Table S2b). Flyers had significantly

321 smaller relative ilium and ischium length optima than other locomotor groups.
322 Gliders+arborealists had metatarsal and intermediate proximal phalanx optima intermediate
323 between flyers and ground-dwellers (Fig. 4d-e; Table S3b). The OUM_{loc3c} model best fit three
324 traits (AICcW = 0.42-0.48): pelvis length, femur distal width, and tibia proximal width (Table
325 S2b). In the latter two traits, gliders exhibited intermediate width optima between flyers (which
326 were smaller) and ground-dwellers+arborealists (where were larger). For pelvis length, like ilium
327 and ischium length, there was no clear trend in the direction of the optima values across
328 locomotor groups (Table S3b).
329 Adding fossil flyers into hindlimb model-fitting analyses yielded only one difference
330 compared to extant-only modeling: pelvis length was now best fit with a OUM_{loc3b} instead of
331 OUM_{loc3c} model (Table S4b). The length and width optima for the hindlimb were very similar
332 between extant+extinct and extant-only modeling (Table S5b).
333

334 Discussion

335 *Forelimb trait evolution*

336 We found evidence that mammalian glider forelimb morphologies are evolving toward
337 adaptive peaks that are intermediate between those of arborealists and flyers. Our multivariate
338 forelimb results and univariate length trait results provide support for the hypothesis that
339 selective pressures for flight influenced the evolution of flyer forelimbs from glider-like
340 forelimbs. Using multivariate evolutionary models, we found a three optima model with distinct
341 selective regimes for ground-dwellers, arborealists+gliders, and flyers as the best fit to the first
342 three PCs of our data (Table 1a). The arborealist+glider optima are intermediate between those
343 of flyers and ground-dwellers (Fig. 2c). PC1 is mostly explained by the variation in the forelimb

344 bone lengths and PC2 by their widths, creating a coarse picture that forelimb bones likely
345 become relatively longer and possibly wider from ground-dwellers to arborealists+gliders to
346 flyers. Results from our univariate evolutionary models are consistent with these findings,
347 revealing that glider forelimb optima are intermediate between flyer and arborealist optima for
348 length traits (Fig. 3a-f), but only partially for width traits (Fig. 3g-j) across both the armwing and
349 handwing (See Table S7 for a breakdown of whether each univariate model supports our
350 hypothesis).

351 Flyers exhibit trait optima indicating evolution of relatively longer forelimb bones
352 compared to all other locomotor groups (Fig. 2a, Fig. 3a-f) particularly in the handwing, which
353 exhibited rapid evolution as a necessary adaptation for bats (Vaughan 1970; Sears et al. 2006;
354 Amador et al. 2019). Increased bone lengths may enhance the surface area of the patagium for
355 greater lift (Norberg 1985b). Flyers also displayed evidence of evolution toward relatively wider
356 bones in the armwing compared to all other locomotor groups (Fig. 3g-j) consistent with findings
357 that bat humeri and radii exhibit significantly larger diameters compared to nonvolant mammals
358 (Swartz and Middleton 2008). These relatively wider proximal forelimb bones combined with
359 thinner yet highly mineralized walls provide resistance to bending and torsion during flapping
360 (Swartz et al. 1992; Papadimitrious et al. 1996). Furthermore, the transition from relatively more
361 robust proximal ends of the humerus to relatively less robust distal ends may also reflect greater
362 muscle mass closer to the center of rotation of the wing joints, which would greatly decrease
363 flight inertial power and facilitate economical flight (Norberg 1985A; Swartz 1997). In the
364 handwing, we found flyers exhibit relatively thicker third metacarpals (Fig. 3j) that corresponded
365 with its relatively increased length (Fig. 3d) compared to nonvolant mammals. In contrast, the
366 proximal phalanx length of the third manual digit was relatively longer compared to nonvolant

mammals whereas its width was best supported with an OU1 model, consistent with previous work showing that the proximal phalanx diameter is not significantly smaller in bats compared to nonvolant mammals (Swartz and Middleton 2008). As a result, bats exhibit relatively thick bone cortices to combat greater bending moments associated with this relatively increased elongation (Swartz et al. 1992; Papadimitriou et al. 1996; Swartz 1997). Increased cortical thickness along with the reduction of mineralization of the handwing work together to resist bending failure while simultaneously maintaining flexibility during flying (Papadimitriou et al. 1996).

In gliders, we found evidence that forelimb bone length optima are largely intermediate between ground-dwellers and flyers. Gliders tend to exhibit relatively greater length optima in most forelimb bones compared to ground-dwelling and arboreal mammals (Thorington and Heaney 1981; Grossnickle et al. 2020; Linden et al. 2023; Rickman et al. 2023) but do not reach the lengths of flyer forelimb bones. Nevertheless, like flyers, the longer bones expand the surface area of the patagium (Thorington and Heaney 1981) and enable further adjustment of their patagium during flight, leading to more efficient aerodynamics, increased agility, and maneuverability (Thorington et al. 1998; Zhao et al. 2019). Forelimb bone widths in gliders, while clearly intermediate between those of ground-dwellers and flyers for some traits (Fig. 3h, i) share an optimum with arborealists (shown by the OUM_{loc3b} support for these traits; Fig. 3g-j) and overlap with ground-dwelling optima mammals for other traits (Fig. 3g, j). Together, these results suggest gliders may maintain high relative widths while continuing to elongate forelimb bones, supporting previous findings that the evolutionary elongation of glider forelimbs is not also accompanied by slimming of the bones (Grossnickle et al. 2020).

389 *Hindlimb trait evolution*

390 We found mixed evidence that mammal glider hindlimb morphologies are intermediate to
391 those of arborealists and flyers. Using our multivariate modeling approach, we found distinct
392 optima for ground-dwellers, arborealists, gliders, and flyers that best fit the first three PCs of our
393 hindlimb data (Table 1b). The trait loadings indicate that the autopodial bones dictate the
394 distribution of PC scores in PCs 1 and 2 (Table S1b). However, there is much overlap among the
395 optima of ground-dwellers, arborealists, and gliders in morphospace (Fig. 2d).

396 The univariate models uncovered further patterns: 1) width optima of hindlimb bones
397 were consistently narrower in flyers and gliders compared to arboreal mammals (Fig. 4f-j), and
398 2) there was no pattern from arboreal to glider to flyer in the hindlimb length optima. Univariate
399 modeling revealed that the widths of hindlimb bones tend not to differ between flyers and gliders
400 (Fig. 4f-j) because the widths of hindlimb bones in flyers and gliders exhibited either a single
401 optimum (i.e., OUM_{loc3a}) separate from ground-dwelling and arboreal mammals (Fig. 4 f, i, j) or
402 an overlap in confidence intervals of optima between flyers and gliders (Fig. 4 g, h). This shared
403 flyer-glider adaptive zone suggests that flyers and gliders exhibit narrower hindlimb optima,
404 especially in the autopod region (Fig. 4f-j). In contrast, univariate modeling revealed distinct
405 optima in long bone lengths of the hindlimb among the four locomotor regimes, in which gliders
406 exhibited relatively longer femoral and tibial optimal lengths compared to flyers, arborealists,
407 and ground-dwellers (Fig. 4b-c). Unlike bat forelimbs, bat long bones in the hindlimb (i.e., the
408 femur and tibia) are not the longest compared to the other locomotor regimes; in fact, the
409 confidence intervals of optimal lengths largely overlap between flyers and arborealists (Table
410 S3b). Furthermore, flyers exhibit relatively shorter metatarsals but relatively longer pedal
411 intermediate phalanges compared to all other locomotor regimes, whereas these autopodial

lengths do not differ between gliders and arborealists (Fig. 4d-e). The different evolutionary patterns of hindlimb bones demonstrate the unique locomotor diversity among the four regimes. Although gliders and flyers are both aerial, these behaviors require different functional morphologies. In gliders, relatively longer hindlimbs are needed to increase the surface area of the patagium in tandem with relatively longer forelimbs to generate lift during gliding (Thorington and Heaney 1981). In contrast, in bats, the relative lengthening of the forelimb supports the majority of the wing membranes whereas the hindlimb, specifically the ankle, serves as an anchor to the wing membrane. Bat hindlimbs are still used for flight by helping modulate lift, drag, or pitch (Cheney et al. 2014).

Overall, gliders appear to be evolving relatively lengthened hindlimb bones while bats are evolving more gracile hindlimb bones. In light of these results, we reject our prediction that flyer and glider hindlimbs overlap in their adaptive optima. This finding may point to the fact that modern gliders are completely distinct evolutionarily and potentially even morphologically from the gliding ancestors of bats. These results may highlight the pitfalls of modeling modern gliders as proxies for ancestral ones instead of invalidating our hypothesis that bats evolved from ancestral gliders.

Incorporating fossil bats

The morphospace positions of fossil bats in the forelimb PCA confirm extinct bats' morphological similarity to extant bats in the degree of forelimb specialization (Fig. 2a). Amador et al. (2019) modeled aerodynamic traits instead of skeletal traits and found that the Eocene bat *Onchonycteris finneyi* occupies an area of aerofoil morphospace between extant gliders and bats.

434 In our morphospace, *O. finneyi* is the closest fossil bat to gliders across PC1 (Fig. S1a),
435 congruent with Amador et al.'s (2019) findings.

436 Fossil flyers occupy the same region of hindlimb morphospace as extant flyers, but three
437 of four species overlap clearly with the region of morphospace of non-flyers, a higher proportion
438 compared to that of extant bats (Fig. 2b). *Tachypteron franzeni* most clearly overlaps with extant
439 flyers and is also the only fossil we included from an extant bat family, Emballonuridae (Storch
440 et al. 2002). Simmons et al. (2008) suggested that, based on its intermediate limb traits,
441 *Onychonycteris finneyi* was likely more proficient at climbing than extant bats and may have
442 employed quadrupedal locomotion and under-branch hanging. Interestingly, *O. finneyi* and
443 *Desmodus rotundus* (the common vampire bat) are almost indistinguishable in the hindlimb
444 morphospace (Fig. S1b). Vampire bats are known for their adept quadrupedal locomotion and
445 climbing (e.g., Riskin et al. 2005), so *O. finneyi'*s similar morphology may lend support to more
446 walking-capable early bats. However, the linear measurements we used here may not reflect the
447 complex adaptations required for these behaviors (e.g., ninety-degree joint rotations for under-
448 branch hanging, Riskin et al. 2005), so the placement of these species in morphospace leaves
449 many possibilities open for ancestral locomotor behaviors.

450 Including fossil flyers in our model-fitting analyses as the closest morphologies we have
451 to flyer-glider intermediaries did not significantly alter estimations of the adaptive zone between
452 flyers and gliders; the inclusion of fossils appeared to make the flyer-glider trait optima
453 marginally more similar for the forelimbs and had no change for the hindlimbs (Table S7). Fossil
454 addition to the multivariate model-fitting analysis shifted support from $mvOUM_{loc3b}$ to
455 $mvOUM_{loc4}$, suggesting that the glider optimum is potentially distancing itself from arborealists'
456 and towards flyers' (Table S6a). Unfortunately, the extant+extinct $mvOUM_{loc4}$ model predicted

extremely negative optima values, which represent unrealistic morphologies that are potentially artifactual, making it difficult to gain more insight into this result (Table S6b). Fossil addition to univariate forelimb model-fitting analyses yielded overall slightly more support for OUM_{loc3a} models compared to extant-only modeling (Table S4a). Fossil addition to hindlimb model-fitting analyses yielded overall no change in support for the $mvOUM_{loc4}$ model or OUM_{loc3a} models compared to extant-only modeling (Table S6, S4b). Regardless, overall the length and width trends are the same as above between locomotor groups across the fore- and hindlimb (Table S5).

Limb trait optima and the adaptive landscape

Our results provide insight on the potential adaptive landscape connecting arboreal, gliding, and flying locomotion (Fig. 5). Overall, we found that glider forelimb optima fall intermediate between those of arborealists and flyers in their lengths but only partially in their widths. Except for long bone lengths, glider hindlimb optima are intermediate between ground-dweller/arborealist and flyer optima or even overlap with flyer optima. Together, these results emphasize that selection on key length/width traits may be "pulling" glider traits towards a flying adaptive zone yet that certain glider traits (e.g., femur and tibia lengths) are derived specifically for gliding morphology. Bishop (2008) proposed that the high degree of convergence among gliders suggests functional constraints on the evolution of powered flight from gliding; however, more recent work found that gliding lineages display incomplete convergence (species retain unique morphologies even while evolving some similarities; Leal et al. 2002; Stayton 2006). For gliders, there is little evidence that gliding is under strong selective pressures toward a single-optimum gliding morphology (Grossnickle et al. 2020). The clustering of bat species in forelimb

480 morphospace (Fig. 2a) may represent a narrow adaptive peak within which forelimb
481 morphologies are highly conserved. In contrast, the broad glider morphospace may represent a
482 gradually inclined selection plane, with gliders still far from a peak (Grossnickle et al. 2020).
483 This broad adaptive slope could represent the foothill of a steep flyer peak such that gliders are
484 very slowly evolving towards a flyer peak (Fig. 5a). The evolutionarily oldest extant glider
485 lineages, dermopterans (colugos) and anomalurids (scaly-tailed squirrels), have evolved farthest
486 from ancestral arborealists (Grossnickle et al. 2020; although some extinct gliders may have
487 experienced relatively greater change from ancestral arborealists, e.g., Meng et al. 2017; Luo et
488 al. 2017). Here, the dermopteran species *Cynocephalus volans* and *Galeopteras variegatus* are
489 the gliders closest to the flyer forelimb region of morphospace (Fig. 3a; Fig. S1a), suggesting a
490 trajectory in morphospace from gliding to flying. Further, colugos are known as the "mitten
491 gliders" because of their interdigital membranes, which, along with their common carpal
492 morphology with bats (Simmons and Geisler 1998), reflects hypotheses that interdigital webbing
493 was key to evolving powered flight (Anderson and Ruxton 2020 but see Gardner and Dececchi
494 2022 for an alternate view).

495 Our results also suggest that both flyers and gliders exhibit broad adaptive optima (i.e.,
496 having large confidence intervals) in the hindlimb due to gliders sharing an optimum or
497 overlapping optima with flyers, or being intermediate between non-flyers and flyers for many
498 traits (Fig. 2d, Fig. 4). These broad adaptive optima could represent overlapping peaks for gliders
499 and flyers separated only by a shallow fitness valley driven by the gliders' elongated femur and
500 tibia lengths (Fig. 5b). The hypothetical adaptive landscape is therefore valuable because the
501 transition from quadrupedalism to hindlimb suspension has been hypothesized to enable
502 forelimbs to evolve more freely since they would no longer be weight-bearing structures (Bishop

503 2008). Indeed, there is both quadrupedal suspension and hindlimb suspension in dermopterans,
504 resulting in a tradeoff in the ability to walk quadrupedally upright (Fujiwara et al. 2011;
505 Granatosky 2018). In the PC1 and PC2 hindlimb morphospace, *G. variegatus* is the only glider
506 that overlaps with the flyer morphologies (Fig. 2b; Fig. S1b), reflecting a hindlimb adaptive
507 optimum potentially more easily attained than that of flyers' specialized forelimbs (Fig. 5).
508 Our modeling approach offers a first step towards support for the hypothesis that
509 selection may more strongly "pull" certain limb traits towards a flyer adaptive zone. In
510 particular, gliders' intermediate forelimb length and overlapping hindlimb width optima between
511 that of arborealists and flyers could be the traits driving lineages across fitness valleys due to
512 their greater effect in, for example, the functionality of the gliding/flying apparatus. However, to
513 complete the tentative adaptive landscape presented here (Fig. 5), these results could be
514 strengthened by more comprehensive coverage of the lengths/widths across more mammal
515 species and biomechanical studies tying these traits to specific functions and selective pressures.
516

517 # Conclusions

518 Our findings complement earlier work investigating the evolution of bat powered flight
519 by testing the selective regimes acting on bone dimensions across the mammalian forelimb and
520 hindlimb. Our results reveal that the relatively lengthened forelimbs in gliders are intermediate to
521 those of bats and arborealists, whereas bats and gliders exhibit similarly relatively narrower
522 hindlimbs compared to arborealists. Thus, solely based on morphometrics, the traditional highly
523 specialized view of glider/bat forelimbs and the "reduced" view of bat hindlimbs may represent
524 more malleable adaptive zones than previously thought. There is a need for future studies to test
525 the biomechanical consequences of such trait optima alongside more synergistic studies taking

526 into account bat and gliders' complex physiology and development to test these hypotheses
527 regarding the evolution of mammalian powered flight.
528

529 **Acknowledgements**

530 We thank Jeff Bradley (UWBM) for extensive access to specimens and Lucas N. Weaver for
531 giving permission for our use of his original skeletal illustrations of *Rattus norvegicus*.
532

533 References

534 Adams, D. C., and M. L. Collyer. 2018. Multivariate phylogenetic comparative methods:
535 evaluations, comparisons, and recommendations. Syst. Biol. 67:14–31.
536 Adams, R. A. 1992. Comparative skeletogenesis of the forearm of the little brown bat (*Myotis*
537 *lucifugus*) and the norway rat (*Rattus norvegicus*). J. Morphol. 214:251–260.
538 Adams, R. A. 2008. Morphogenesis in bat wings: linking development, evolution and ecology.
539 Cells Tissues Organs 187:13–23.
540 Adams, R. A., and J. B. Shaw. 2013. Time's arrow in the evolutionary development of bat flight.
541 Pp. 21–46 *in* R. A. Adams and S. C. Pedersen, eds. Bat Evolution, Ecology, and
542 Conservation. Springer New York, New York, NY.
543 Álvarez-Carretero, S., A. U. Tamuri, M. Battini, F. F. Nascimento, E. Carlisle, R. J. Asher, Z.
544 Yang, P. C. J. Donoghue, and M. dos Reis. 2022. A species-level timeline of mammal
545 evolution integrating phylogenomic data. Nature 602:263–267.
546 Amador, L. I., N. B. Simmons, and N. P. Giannini. 2019. Aerodynamic reconstruction of the
547 primitive fossil bat *Onychonycteris finneyi* (Mammalia: Chiroptera). Biol. Lett.
548 15:20180857.

549 Anderson, S. C., and G. D. Ruxton. 2020. The evolution of flight in bats: a novel hypothesis.
550 Mammal Rev. 50:426–439.
551 Anthwal, N., D. J. Urban, A. Sadier, R. Takenaka, S. Spiro, N. Simmons, R. R. Behringer, C. J.
552 Cretekos, J. J. Rasweiler, and K. E. Sears. 2023. Insights into the formation and
553 diversification of a novel chiropteran wing membrane from embryonic development.
554 BMC Biology 21:101.
555 Beaulieu, J. M., D.-C. Jhwueng, C. Boettiger, and B. C. O'Meara. 2012. Modeling stabilizing
556 selection: Expanding the Ornstein-Uhlenbeck model of adaptive evolution. Evolution
557 66:2369–2383.
558 Bishop, K. L. 2008. The evolution of flight in bats: narrowing the field of plausible hypotheses.
559 Q. Rev. Biol. 83:153–169.
560 Boettiger, C., G. Coop, and P. Ralph. 2012. Is your phylogeny informative? Measuring the
561 power of comparative methods. Evolution 66:2240–2251.
562 Butler, M. A., and A. A. King. 2004. Phylogenetic comparative analysis: a modeling approach
563 for adaptive evolution. Am. Nat. 164:683–695.
564 Caple, G., R. P. Balda, and W. R. Willis. 1983. The physics of leaping animals and the evolution
565 of preflight. Am. Nat. 121:455–476.
566 Cartmill, M. 1985. Chapter 5. Climbing. Pp. 73–88 *in* M. Hildebrand, D. M. Bramble, K. F.
567 Liem, and D. B. Wake, eds. Functional Vertebrate Morphology. Harvard University
568 Press.
569 Chen, M., and G. P. Wilson. 2015. A multivariate approach to infer locomotor modes in
570 Mesozoic mammals. Paleobiology 41:280–312.
571 Cheney, J. A., N. Konow, K. M. Middleton, K. S. Breuer, T. J. Roberts, E. L. Giblin, and S. M.

572 Swartz. 2014. Membrane muscle function in the compliant wings of bats. Bioinspir.
573 Biomim. 9:025007. IOP Publishing.
574 Clavel, J., G. Escarguel, and G. Merceron. 2015. mvMORPH:anR package for fitting
575 multivariate evolutionary models to morphometric data. Methods Ecol Evol 6:1311–
576 1319.
577 Cooper, K. L., and C. J. Tabin. 2008. Understanding of bat wing evolution takes flight. Genes
578 Dev. 22:121–124.
579 Farnum, C. E., M. Tinsley, and J. W. Hermanson. 2008. Forelimb versus hindlimb skeletal
580 development in the Big Brown Bat, *Eptesicus fuscus:* functional divergence is reflected
581 in chondrocytic performance in autopodial growth plates. Cells Tissues Organs 187:35–
582 47.
583 Feigin, C. Y., J. A. Moreno, R. Ramos, S. A. Mereby, A. Alivisatos, W. Wang, R. van
584 Amerongen, J. Camacho, J. J. Rasweiler, R. R. Behringer, B. Ostrow, M. V. Plikus, and
585 R. Mallarino. 2023. Convergent deployment of ancestral functions during the evolution
586 of mammalian flight membranes. Science Advances 9:eade7511. American Association
587 for the Advancement of Science.
588 Fujiwara, S., H. Endo, and J. R. Hutchinson. 2011. Topsy-turvy locomotion: biomechanical
589 specializations of the elbow in suspended quadrupeds reflect inverted gravitational
590 constraints: Elbow mechanics in suspended quadrupeds. J. Anat. 219:176–191.
591 Gardner, N. M., and T. A. Dececchi. 2022. Flight and echolocation evolved once in Chiroptera:
592 comments on 'The evolution of flight in bats: a novel hypothesis.' Mammal Rev. 52:284–
593 290.
594 Giannini, N. P. 2012. Toward an integrative theory on the origin of bat flight. Pp. 353–384 *in* G.

595 F. Gunnell and N. B. Simmons, eds. Evolutionary History of Bats. Cambridge University
596 Press, Cambridge.
597 Granatosky, M. C. 2018. Forelimb and hindlimb loading patterns during quadrupedal locomotion
598 in the large flying fox (*Pteropus vampyrus*) and common vampire bat (*Desmodus*
599 *rotundus*). J. Zool. 305:63–72.
600 Grossnickle, D. M., M. Chen, J. G. A. Wauer, S. K. Pevsner, L. N. Weaver, Q.-J. Meng, D. Liu,
601 Y.-G. Zhang, and Z.-X. Luo. 2020. Incomplete convergence of gliding mammal
602 skeletons. Evolution 74:2662–2680.
603 Gunnell, G. F., and N. B. Simmons. 2005. Fossil Evidence and the Origin of Bats. J. Mamm.
604 Evol. 12:209–246.
605 Hallgrímsson, B., K. Willmore, and B. K. Hall. 2002. Canalization, developmental stability, and
606 morphological integration in primate limbs. Am. J. Phys. Anthropol. Suppl 35:131–158.
607 Hansen, T. F. 1997. Stabilizing selection and the comparative analysis of adaptation. Evolution
608 51:1341–1351.
609 Heard, S. B., and D. L. Hauser. 1995. Key evolutionary innovations and their ecological
610 mechanisms. Hist. Biol. 10:151–173.
611 Hildebrand, M. 1985. Chapter 6. Digging of Quadrupeds. Pp. 89–109 *in* M. Hildebrand, D. M.
612 Bramble, K. F. Liem, and D. B. Wake, eds. Functional Vertebrate Morphology. Harvard
613 University Press.
614 Hunter, J. P. 1998. Key innovations and the ecology of macroevolution. Trends Ecol. Evol.
615 13:31–36.
616 Jetz, W., G. H. Thomas, J. B. Joy, K. Hartmann, and A. O. Mooers. 2012. The global diversity of
617 birds in space and time. Nature 491:444–448.

Jones, K. E., J. Bielby, M. Cardillo, S. A. Fritz, J. O'Dell, C. D. L. Orme, K. Safi, W. Sechrest, E. H. Boakes, C. Carbone, C. Connolly, M. J. Cutts, J. K. Foster, R. Grenyer, M. Habib, C. A. Plaster, S. A. Price, E. A. Rigby, J. Rist, A. Teacher, O. R. P. Bininda-Emonds, J. L. Gittleman, G. M. Mace, and A. Purvis. 2009. PanTHERIA: a species-level database of life history, ecology, and geography of extant and recently extinct mammals. Ecology 90:2648–2648.

Kurochkin, E. N., and I. A. Bogdanovich. 2010. Origin of feathered flight. Paleontol. J. 44:1570–1588.

Leal, M., A. K. Knox, and J. B. Losos. 2002. Lack of Convergence in Aquatic Anolis Lizards. Evolution 56:785–791.

Linden, T. J., A. E. Burtner, J. Rickman, A. McFeely, S. E. Santana, and C. J. Law. 2023. Scaling patterns of body plans differ among squirrel ecotypes. PeerJ 11:e14800. PeerJ Inc.

Long, C. A., G. P. Zhang, T. F. George, and C. F. Long. 2003. Physical theory, origin of flight, and a synthesis proposed for birds. J. Theor. Biol. 224:9–26.

Luo, Z.-X., Meng, Q.-J., Grossnickle, D. M., Liu, D., Zhang, Y.-G., Neander, A. I., and Q, Ji. 2017. New evidence for mammaliaform ear evolution and feeding adaptation in a Jurassic ecosystem. Nature. 548: 326-329 (doi:10.1038/nature23483).

Louzada, N. S. V., M. R. Nogueira, and L. M. Pessôa. 2019. Comparative morphology and scaling of the femur in yangochiropteran bats. J. Anat. joa.12996.

Meng, Q.-J., Grossnickle, D. M., Liu, D., Zhang, Y.-G., Neander, A. I., Ji, Q., and Z.-X. Luo. 2017. New gliding mammaliaforms from the Jurassic. Nature. 548: 291-296. (doi:10.1038/nature23476).

Mosimann, J. E. 1970. Size Allometry: Size and Shape Variables with Characterizations of the Lognormal and Generalized Gamma Distributions. J. Am. Stat. Assoc. 65:930–945.

Nicholson, D. B., A. J. Ross, and P. J. Mayhew. 2014. Fossil evidence for key innovations in the evolution of insect diversity. Proc. R. Soc. B Biol. Sci. 281:20141823. Royal Society.

Nojiri, T., I. Werneburg, V. T. Tu, D. Fukui, M. Takechi, S. Iseki, T. Furutera, and D. Koyabu. 2023. Timing of organogenesis underscores the evolution of neonatal life histories and powered flight in bats. Proc. R. Soc. B Biol. Sci. 290:20221928. Royal Society.

Norberg, U. M. 1985. Chapter 8. Flying, Gliding, and Soaring. Pp. 148–152 *in* M. Hildebrand, D. M. Bramble, K. F. Liem, and D. B. Wake, eds. Functional Vertebrate Morphology. Harvard University Press.

Norberg, U. M. 1985. Evolution of Vertebrate Flight: An Aerodynamic Model for the Transition from Gliding to Active Flight. Am. Nat. 126:303–327. [University of Chicago Press, American Society of Naturalists].

Norberg, U. M. 1990. Vertebrate Flight. Springer Berlin Heidelberg, Berlin, Heidelberg.

Padian, K. 1982. Running, Leaping, Lifting Off. The Sciences 22:10–15.

Papadimitriou, H. M., S. M. Swartz, and T. H. Kunz. 1996. Ontogenetic and anatomic variation in mineralization of the wing skeleton of the Mexican free-tailed bat, Tadarida brasiliensis. Journal of Zoology 240:411–426.

Pevsner, S. K., D. M. Grossnickle, and Z.-X. Luo. 2022. The functional diversity of marsupial limbs is influenced by both ecology and developmental constraint. Biol. J. Linn. Soc. 135:569–585.

R Core Team. 2021. R: A language and environment for statistical computing. Foundation for Statistical Computing, Vienna, Austria.

Revell, L. J. 2012. phytools: an R package for phylogenetic comparative biology (and other things). Methods Ecol. Evol. 3:217–223.

Rickman, J., A. E. Burtner, T. J. Linden, S. E. Santana, and C. J. Law. 2023. Size And Locomotor Ecology Have Differing Effects on the External and Internal Morphologies of Squirrel (Rodentia: Sciuridae) Limb Bones. Integrative Organismal Biology 5:obad017.

Riskin, D. K., J. E. A. Bertram, and J. W. Hermanson. 2005. Testing the hindlimb-strength hypothesis: non-aerial locomotion by Chiroptera is not constrained by the dimensions of the femur or tibia. J. Exp. Biol. 208:1309–1319.

Schneider, C. A., W. S. Rasband, and K. W. Eliceiri. 2012. NIH Image to ImageJ: 25 years of image analysis. Nat. Methods 9:671–675.

Sears, K. E., R. R. Behringer, J. J. Rasweiler, and L. A. Niswander. 2006. Development of bat flight: Morphologic and molecular evolution of bat wing digits. Proc. Natl. Acad. Sci. 103:6581–6586.

Simmons, N. B., and A. L. Cirranello. 2022B. Bat Species of the World: A taxonomic and geographic database.

Simmons, N. B., and J. H. Geisler. 1998. Phylogenetic relationships of Icaronycteris, Archaeonycteris, Hassianycteris, and Palaeochiropteryx to extant bat lineages, with comments on the evolution of echolocation and foraging strategies in Microchiroptera. Bulletin of the AMNH ; no. 235. Relationships of Eocene bats. [New York] : American Museum of Natural History.

Simmons, N. B., K. L. Seymour, J. Habersetzer, and G. F. Gunnell. 2008. Primitive Early Eocene bat from Wyoming and the evolution of flight and echolocation. Nature 451:818–821.

687 Smith, J. D. 1977. Comments on Flight and the Evolution of Bats. Pp. 427–437 *in* M. K. Hecht,
688 P. C. Goody, and B. M. Hecht, eds. Major Patterns in Vertebrate Evolution. Springer US,
689 Boston, MA.
690 Stayton, C. T. 2006. Testing hypotheses of convergence with multivariate data: morphological
691 and functional convergence among herbivorous lizards. Evolution 60:824–841.
692 Storch, G., B. Sigé, and J. Habersetzer. 2002. Tachypteron franzeni n. gen., n. sp., earliest
693 emballonurid bat from the Middle Eocene of Messel (Mammalia, Chiroptera). Paläontol.
694 Z. 76:189–199.
695 Swartz, S. M., M. B. Bennett, and D. R. Carrier. 1992. Wing bone stresses in free flying bats and
696 the evolution of skeletal design for flight. Nature 359:726–729.
697 Swartz, S. M. 1997. Allometric patterning in the limb skeleton of bats: Implications for the
698 mechanics and energetics of powered flight. J Morphol 234:277–294.
699 Swartz, S. M., and K. M. Middleton. 2008. Biomechanics of the bat limb skeleton: scaling,
700 material properties and mechanics. Cells Tissues Organs 187:59–84.
701 Teeling, E. C., M. Scally, D. J. Kao, M. L. Romagnoli, M. S. Springer, and M. J. Stanhope.
702 2000. Molecular evidence regarding the origin of echolocation and ¯ight in bats. 403:5.
703 Thorington, R. W., and L. R. Heaney. 1981. Body proportions and gliding adaptations of flying
704 squirrels (Petauristinae). J. Mammal. 62:101–114.
705 Thorington, R. W., K. Darrow, and C. G. Anderson. 1998. Wing Tip Anatomy and
706 Aerodynamics in Flying Squirrels. Journal of Mammalogy 79:245–250. [American
707 Society of Mammalogists, Oxford University Press].
708 Thorington, R. W., and E. M. Santana. 2007. How to make a flying squirrel: *Glaucomys* anatomy
709 in phylogenetic perspective. J. Mammal. 88:882–896.

Upham, N. S., J. A. Esselstyn, and W. Jetz. 2019. Inferring the mammal tree: Species-level sets of phylogenies for questions in ecology, evolution, and conservation. PLoS Biol. 17:e3000494.

Uyeda, J. C., D. S. Caetano, and M. W. Pennell. 2015. Comparative analysis of principal components can be misleading. Syst. Biol. 64:677–689.

Vaughan, T. A. 1970. Vaughan, T. A. (1970). The skeletal system. In Biology of Bats 1, ed. W. A. Wimsatt. New York: Academic Press. pp. 98–139. Pp. 98–139 *in* Biology of Bats. New York: Academic Press.

Weaver, L. N., and D. M. Grossnickle. 2020. Functional diversity of small-mammal postcrania is linked to both substrate preference and body size. Curr. Zool. 66:539–553.

Wilson, and R. A. Mittermeier. 2009. Handbook of the Mammals of the World. Wilson&R. A. Mittermeier, Eds. Lynx Edicions.

Young, N. M., and B. Hallgrímsson. 2005. Serial homology and the evolution of mammalian limb covariation structure. Evolution 59:2691–2704.

Zhao, F., W. Wang, J. Zhang, J. Wyrwa, and F. Sun. 2019. Aerodynamic Characteristics and Pitching Adjusting Mechanism of the Flying Squirrel With Deployed Patagium. IEEE Access 7:185554–185564.

Figure Captions

Fig. 1. Morphological measurements and phylogeny. We conducted analyses based on this a) phylogeny (Upham et al. 2019) across b) 14 forelimb linear measurements for each specimen of scapula height and length (sh, sl), humerus length (hl), distal width (hdw), proximal width (hpw), and mid-shaft width (hsw), radius length (rl), ulna length and olecranon length (ul, uol), and third

manual digit metacarpal length and width (mcl, mcw), proximal phalanx length and width (ppl, ppw), and intermediate phalanx length (ipl) and we collected c) 15 hind limb measurements consisted of pelvis, ilium, and ischium length (pel, il, isl); femur length (fl), distal width (fdw), and midshaft width (fsw); tibia length (tl), proximal length (tpw), and midshaft width (tmw); fibula length (fbl), and third pedal digit metatarsal length and width (mtl, mtw), proximal phalanx length and width (ppxl, ppxw), and intermediate phalanx length (ipxl). We measured only the third digit in this dataset (and not, for example, the fifth even though that might be of biological interest) in order to build on previous datasets in the literature to generate a large enough dataset for evolutionary modeling.

Fig. 2. Forelimb and hind limb PCAs. Morphospaces consist of PC1 and PC2 of 14 forelimb traits (left panels) and 15 hind limb traits (right panels). The extant+extinct morphospace is shown for the a) forelimbs and b) hind limbs. The extant-only morphospace of c) the mvOUMloc3b optima (large icons) overlaid on the forelimb morphospace and the d) the mvOUMloc4 optima (large icons) overlaid on the hind limb morphospace. Cartoons of a e) quadrupedal mammal skeleton (Rattus norvegicus) versus a f) bat skeleton (Pipistrellus abramus are shown where dark gray shaded bones on the cartoon skeletons correspond to those measured to generate the morphospace.

Fig. 3. Forelimb trait optima from model-fitting of univariate traits. Forelimb OUM optima (θ) as a size-corrected trait value (log-shape ratio) with 95% confidence intervals (Tables S3a) for the best-fitting models (ΔAIC = 0) for 10 traits. The AICcW of the model is on top of each panel (Table S2a).

Fig. 4. Hind limb trait optima from model-fitting of univariate traits. Hind limb OUM optima (θ) as a size-corrected trait value (log-shape ratio) with 95% confidence intervals (Tables S3b) for the best-fitting models (ΔAIC = 0) for 10 traits. The AICcW of the model is on top of each panel (Table S2b).

Fig. 5. Hypothetical adaptive landscapes of forelimb and hind limb skeletal relative length and width evolution. Hypothetical fitness peaks are shown for arborealists, gliders, and bats for a broad summary of our conclusions from the skeletal trait optima results discussed. The "length" and "width" in the figure refer to the lengths and widths of individual limb elements. For the a) forelimb, we depict arborealists on a relatively steep adaptive peak at relatively lower length/width optima, gliders on a broad, shallow peak/incline at relatively higher length but not width optima, and bats on a very steep peak at relatively higher length and width optima. For the b) hind limb, we depict arborealists again on a fairly steep adaptive peak at relatively higher width but not length optima, bats on a shallow steep peak at relatively higher length and lower width optima, and gliders on a peak similar to and overlapping with bats' at relatively higher length but similar width optima.

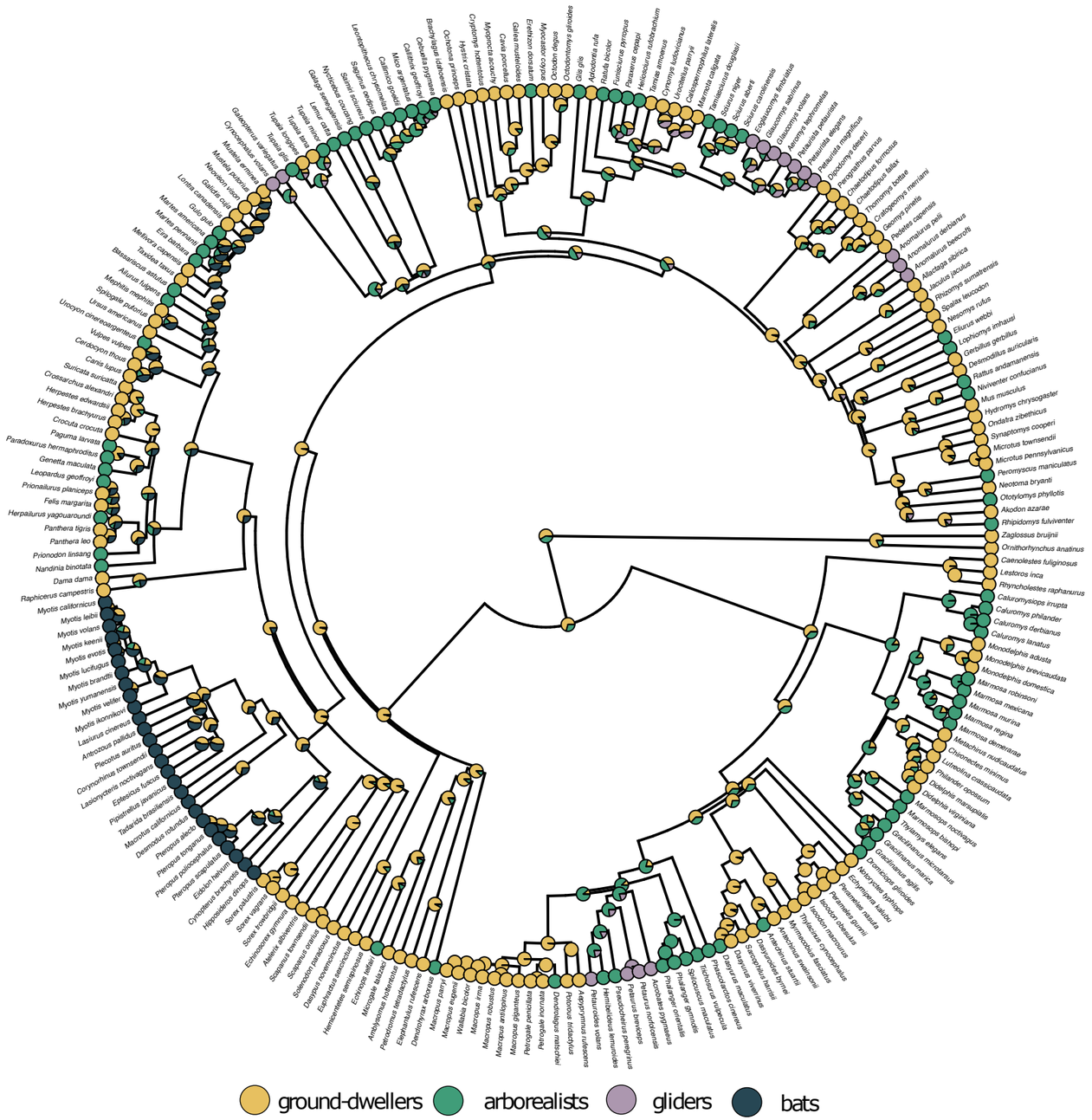
ground-dwellers
arborealists
gliders
bats

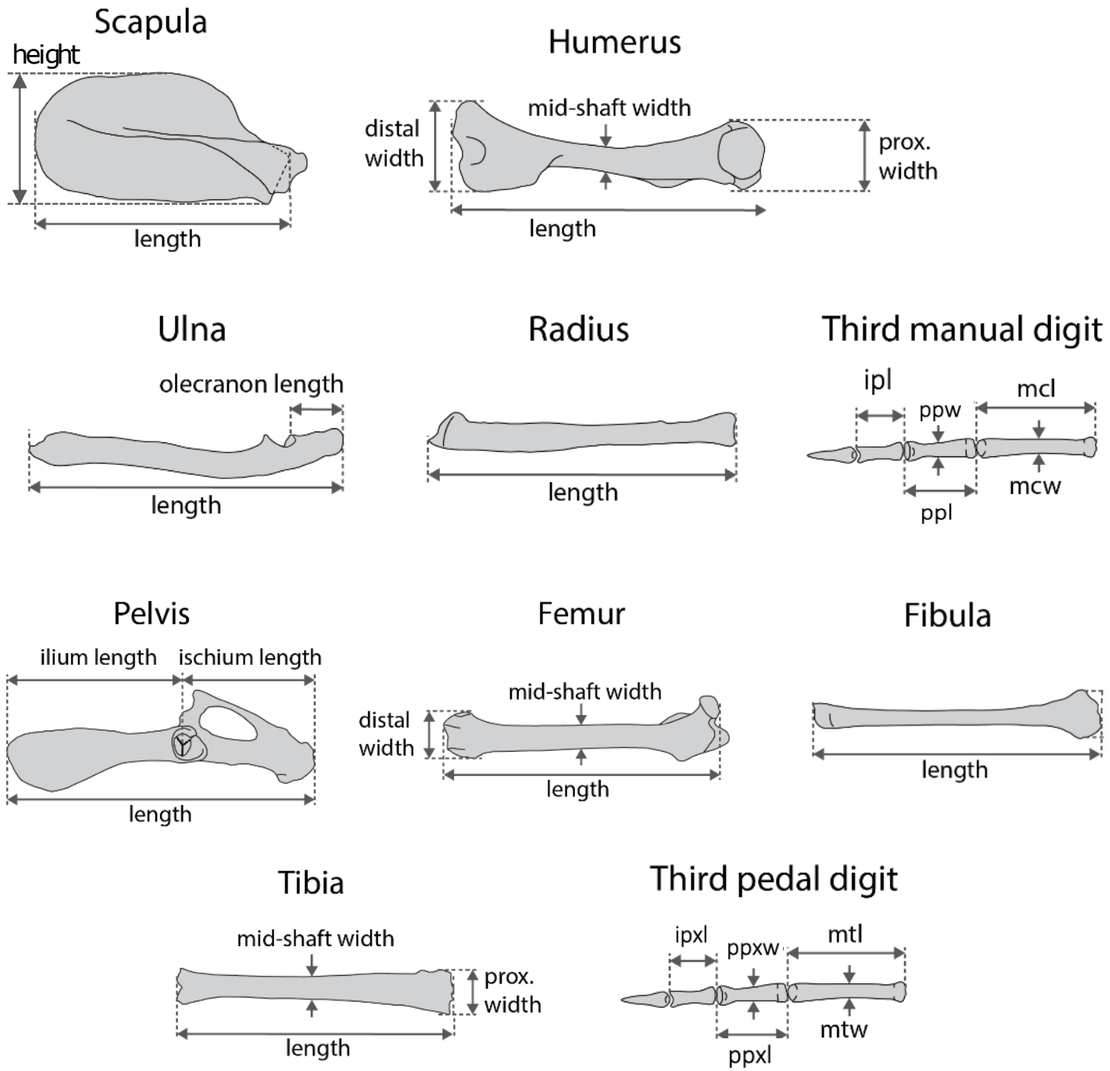
Scapula
height
length
Humerus
distal width
mid-shaft width
prox. width
length
Ulna
olecranon length
length
Radius
length
Third manual digit
ipl
ppw
mcl
mcw
ppl
Pelvis
ilium length
ischium length
length
Femur
distal width
mid-shaft width
length
Fibula
length
Tibia
mid-shaft width
prox. width
length
Third pedal digit
ipxl
ppxw
mtl
mtw
ppxl

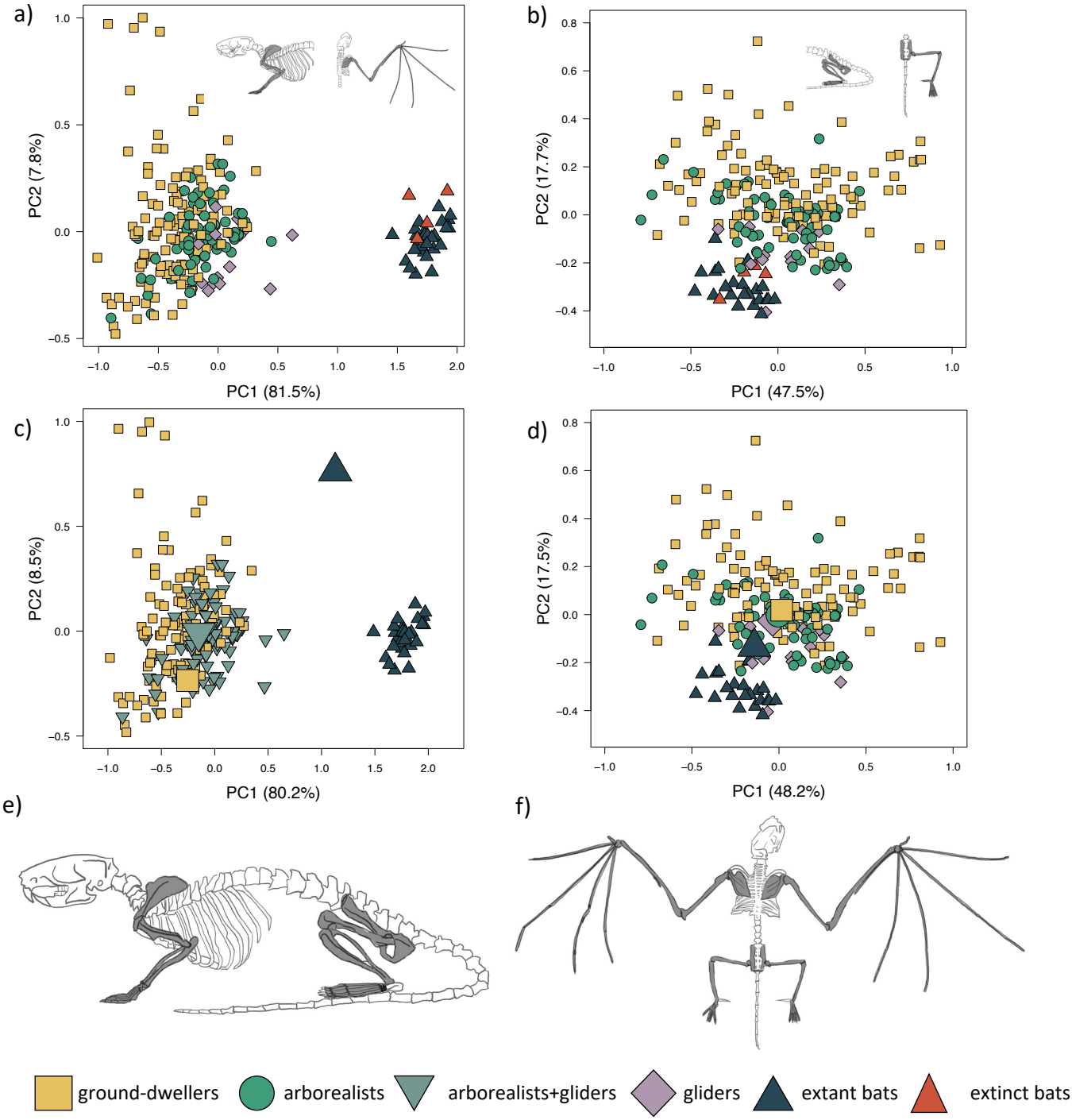
a)
PC2 (7.8%)
PC1 (81.5%)
b)
PC2 (17.7%)
PC1 (47.5%)
c)
PC2 (8.5%)
PC1 (80.2%)
d)
PC2 (17.5%)
PC1 (48.2%)
e)
f)
ground-dwellers
arborealists
arborealists+gliders
gliders
extant bats
extinct bats

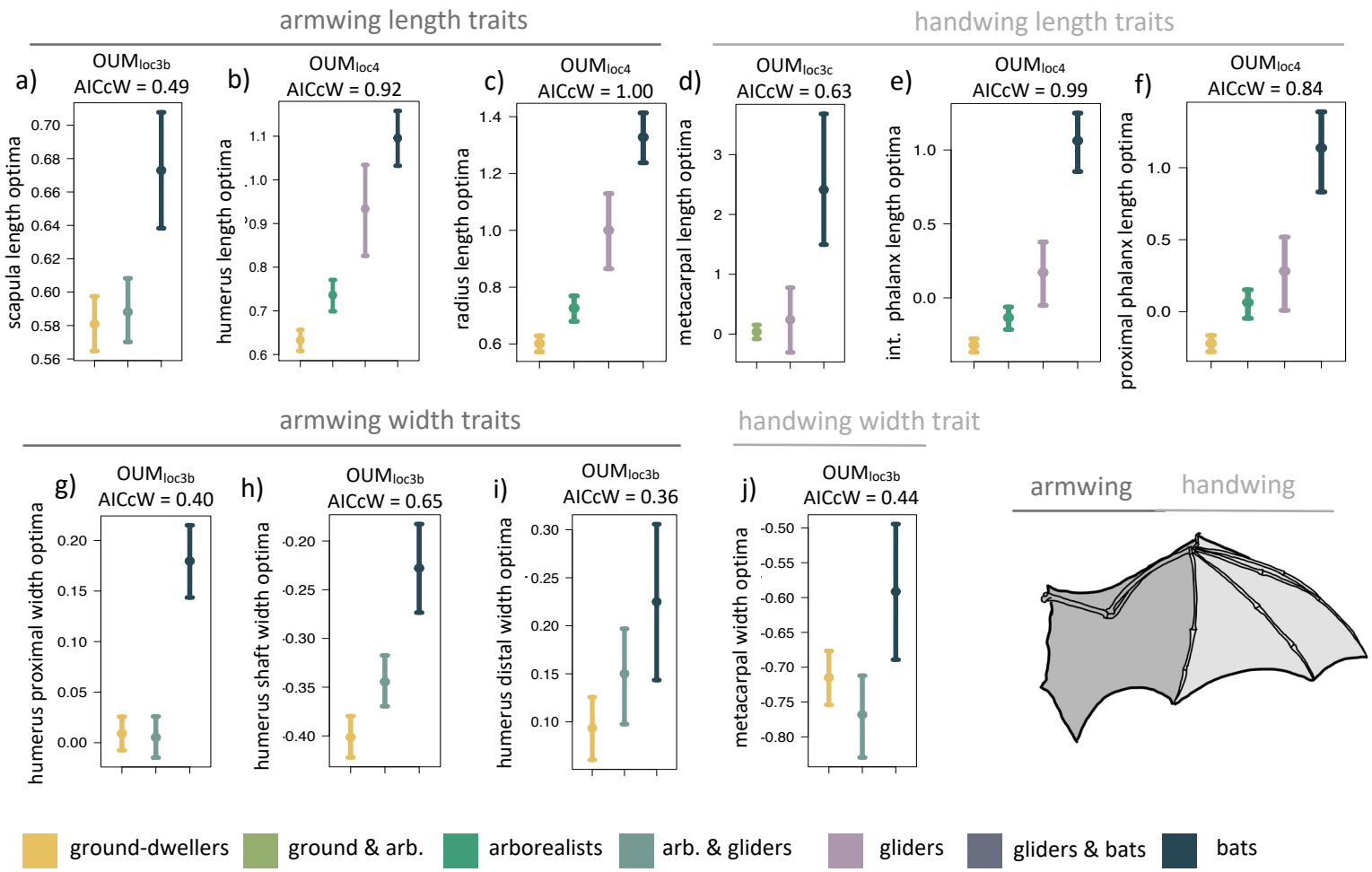
armwing length traits
handwing length traits
a)
OUMloc3b
AICcW = 0.49
scapula length optima
b)
OUMloc4
AICcW = 0.92
humerus length optima
c)
OUMloc4
AICcW = 1.00
radius length optima
d)
OUMloc3c
AICcW = 0.63
metacarpal length optima
e)
OUMloc4
AICcW = 0.99
int. phalanx length optima
f)
OUMloc4
AICcW = 0.84
proximal phalanx length optima
armwing width traits
handwing width trait
g)
OUMloc3b
AICcW = 0.40
humerus proximal width optima
h)
OUMloc3b
AICcW = 0.65
humerus shaft width optima
i)
OUMloc3b
AICcW = 0.36
humerus distal width optima
j)
OUMloc3b
AICcW = 0.44
metacarpal width optima
armwing
handwing
ground-dwellers
ground & arb.
arborealists
arb. & gliders
gliders
gliders & bats
bats

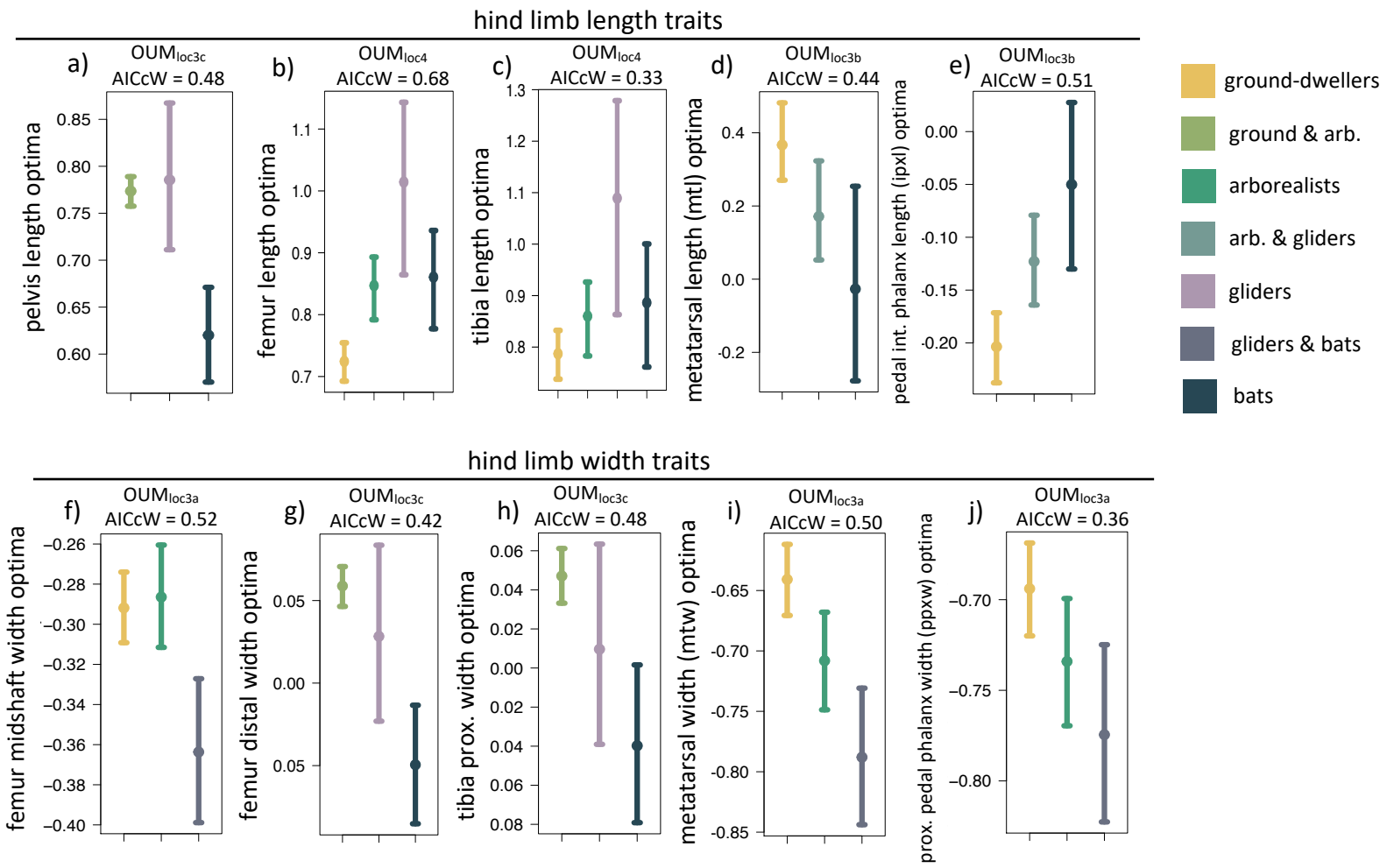
hind limb length traits
a)
OUMloc3c
AICcW = 0.48
pelvis length optima
b)
OUMloc4
AICcW = 0.68
femur length optima
c)
OUMloc4
AICcW = 0.33
tibia length optima
d)
OUMloc3b
AICcW = 0.44
metatarsal length (mtl) optima
e)
OUMloc3b
AICcW = 0.51
pedal int. phalanx length (ipxl) optima
ground-dwellers
ground & arb.
arborealists
arb. & gliders
gliders
gliders & bats
bats
hind limb width traits
f)
OUMloc3a
AICcW = 0.52
femur midshaft width optima
g)
OUMloc3c
AICcW = 0.42
femur distal width optima
h)
OUMloc3c
AICcW = 0.48
tibia prox. width optima
i)
OUMloc3a
AICcW = 0.50
metatarsal width (mtw) optima
j)
OUMloc3a
AICcW = 0.36
prox. pedal phalanx width (ppxw) optima

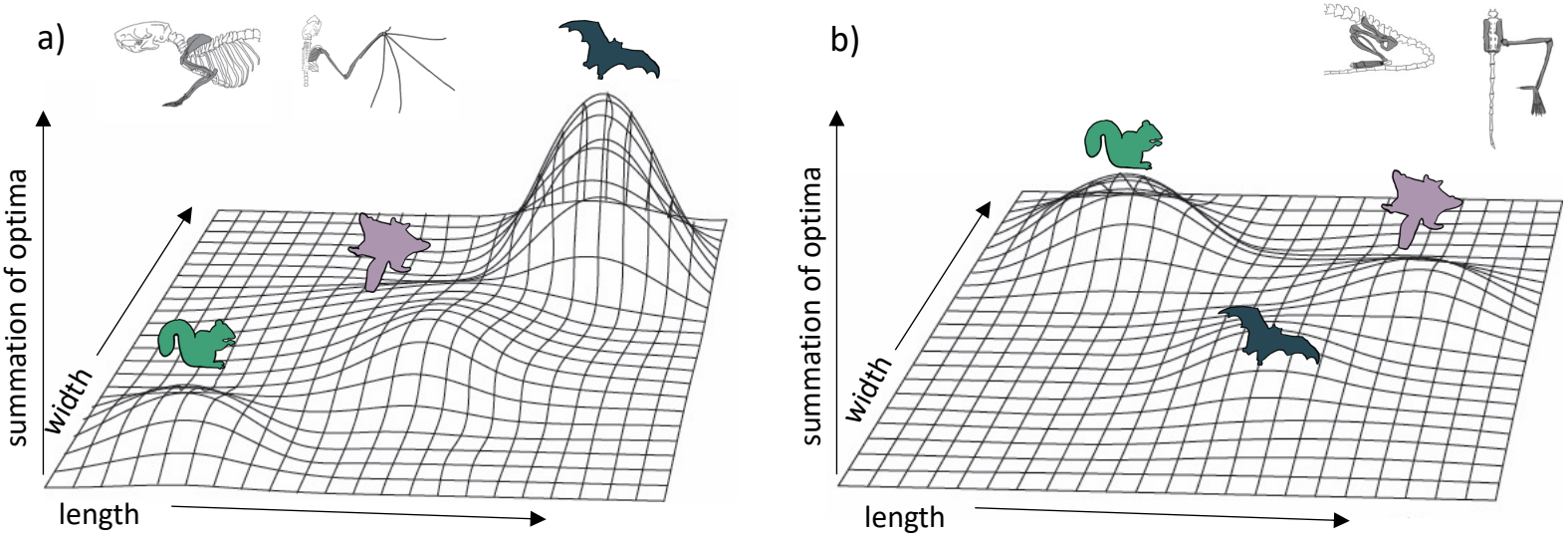
a)
summation of optima
width
length
b)
summation of optima
width
length

Table 1: AICcW scores from multivariate model-fitting analyses (via mvMORPH). Comparisons of the fits of multivariate models to the first three principal components of the a) forelimb dataset and b) hindlimb dataset.

a) forelimb	AIC	ΔAICc	mAICcW	**b) hindlimb**	AIC	ΔAICc	mAICcW
mvBM1	-94.42	225.50	0.00	mvBM1	-134.64	230.05	0.00
mvOU1	-248.73	71.20	0.00	mvOU1	-330.72	33.97	0.00
$mvOUM_{loc3a}$	-306.82	13.10	0.00	$mvOUM_{loc3a}$	-358.41	6.28	0.04
$mvOUM_{loc3b}$	**-319.93**	**0.00**	**0.99**	$mvOUM_{loc3b}$	-353.51	11.17	0.00
$mvOUM_{loc3c}$	-308.77	11.16	0.00	$mvOUM_{loc3c}$	-358.10	6.59	0.03
$mvOUM_{loc4}$	-302.35	17.57	0.00	**$mvOUM_{loc4}$**	**-364.69**	**0.00**	**0.92**